NONLINEAR CONTROL OF LARGE DISTURBANCES IN
MAGNETIC BEARING SYSTEMS

Yuhong Jiang and R. B. Zmood

Department of Electrical Engineering
Royal Melbourne Institute of Technology
Melbourne Victoria 3000, Australia

SUMMARY

In this paper, the nonlinear operation of magnetic bearing control methods is reviewed. For large disturbances, the effects of displacement constraints and power amplifier current and di/dt limits on bearing control system performance are analyzed. The operation of magnetic bearings exhibiting self-excited large scale oscillations have been studied both experimentally and by simulation. The simulation of the bearing system has been extended to include the effects of eddy currents in the actuators, so as to improve the accuracy of the simulation results. The results of these experiments and simulations are compared, and some useful conclusions are drawn for improving bearing system robustness.

1. INTRODUCTION

A magnetic bearing system with a long thin shaft can often have self-excited instabilities, especially when the shaft rotates at high speed. These instabilities can lead to severe rotor vibrations. This problem has been studied by many researchers using the H^∞, root locus, PID, and LQG methods (refs. 1, 2, and 3), for designing stable controllers using linearized models of the magnetic bearings and these approaches have been shown to give excellent results when the transient disturbances are small. However, due to bearing actuator nonlinearities and constraints, and particularly due to power amplifier nonlinearities, the above methods have proven to give poor robustness when the system is subjected to large disturbances.

The effects of nonlinear control of large disturbances in magnetic bearing systems have been studied in an earlier unpublished memorandum by Zmood et. al. (ref. 4). This analysis showed

305

that large scale self-excited oscillations can occur, and these results have been found to be due to a limit cycle which occurs in the bearing control system. This study indicated that reduction of the bearing control winding inductance not only allowed easier adjustment of the controller coefficients for stability but also significantly improved the bearing robustness in the presence of large disturbances. That work, however, did not include the effects of the eddy currents in either the bearing actuator or power amplifier models.

The present work is an extension of this earlier work of Zmood et. al. (ref. 4). The simulation of the magnetic bearing system has been extended to include the effects of the eddy currents in the power amplifier and the bearing actuator. Both transfer functions modelling eddy currents are first order. In this comparison, the results of the simulation using the eddy current models predict the experimental results more accurately. Some new useful design constraints are also derived for improving the magnetic bearing stability and robustness, such as the coil inductance, the height of the solid core of linear ferromagnetic material, and the gain coefficient. The results of the simulation and experimental work have shown that taking into account the system constraints in the controller design not only improves the large signal behaviour of the bearing and prevents self-excited oscillations, but also significantly improves its robustness.

2. MODEL OF THE MAGNETIC BEARING SYSTEM

To aid in understanding the bearing relaxation oscillation, it has been found necessary to make a number of simplifying assumptions about both the bearing actuator and the control system. While some of these assumptions have only a minor influence on the operation of the magnetic bearing, others limit the range of operating conditions which can be described.

2.1 The Magnetic Bearing Actuator

It will be assumed in developing a model for the bearing actuator that :

- The back e.m.f. induced in the actuator coils can be neglected;
- The coil resistance can be neglected;
- Eddy currents induced in the ferromagnetic components of the actuator are represented by a first order model;
- Magnetic saturation can be neglected;
- When the flywheel collides with the touchdown bearings the velocity immediately falls to zero;

- The actuator force is described by the equation $F_x = K_x x + K_i i_c$, where K_x and K_i are both positive;

Under the above assumptions, the equation of motion for the magnetic bearing are given by the following three conditions:

(1) When $-x_m < x(t) < x_m$, the equations of motion are given by

$$M\frac{d^2x}{dt^2} = k_i i_c - k_x x \qquad (1)$$

$$L\frac{di_c}{dt} = V_c(t) \qquad (2)$$

(2) When $x(t) = x_m$ and $i_c(t) > -i_{crit}$, or $x(t) = -x_m$ and $i_c(t) < i_{crit}$, the equations of motion are

$$\frac{dx}{dt} = 0 \qquad (3)$$

$$L\frac{di_c}{dt} = V_c(t) \qquad (4)$$

(3) When $x(t) = x_m$ and $i_c(t) \leq -i_{crit}$, or $x(t) = -x_m$ and $i_c(t) \geq i_{crit}$, the equations of motion are given by

$$M\frac{d^2x}{dt^2} = k_i i_c - k_x x \qquad (5)$$

$$L\frac{di_c}{dt} = V_c(t) \qquad (6)$$

where x is the journal displacement of the shaft and i_c is the coil current. For the above equations, the critical current is defined as $i_{crit} = k_x x_m / k_i$

2.2. Control System Block Diagram

A detailed block diagram for the magnetic bearing control is shown in Fig. 1. This figure shows the parameters for the compensator, low pass filter, and position transducer.
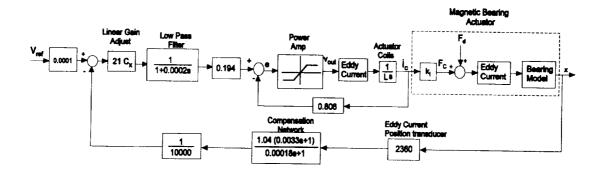

Figure 1. Detailed block diagram of magnetic bearing control system.

3. MODEL OF THE EDDY CURRENTS ON MAGNETIC BEARING ACTUATOR AND POWER AMPLIFIER

Eddy currents are to be found in any conductive material which is subjected to a time-varying magnetic field, and they therefore occur in all types of electrical equipment (ref. 5). In the magnetic bearing control system, the simulations more accurately predict the system performance when models of the eddy currents are included. The details of the eddy current transfer function models are described below.

3.1 Eddy Currents on the Magnetic Bearing Actuator

A first order transfer function model, describing the effects of the eddy currents on the transient performance of a magnetic bearing actuator, was presented by Zmood et. al. (ref. 6). In that paper, the transfer function of the bearing actuator was shown to be

$$F(s) = -K_x x(s) + K_i \frac{1 + s(1 - 8/\pi)T_1}{1 + sT_1} i_c(s)$$

(7)

This equation shows the functional relationship between the armature force $F(s)$, the armature displacement $x(s)$, and the coil current $i_c(s)$. The effect of the eddy currents is to introduce a

time-lag in the application of the force due to change in the coil currents. A block diagram for the bearing actuator including the armature mass is shown in Fig. 2.
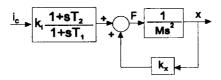

Figure 2. Block diagram of bearing actuator including eddy currents.

From Eq. (7), the transfer function representing the eddy currents in the bearing actuator can be seen to be

$$G_m(s) = \frac{1 + T_2 s}{1 + T_1 s} = \frac{1 + 0.3085s}{1 + 0.1636 \times 10^{-3} s}$$

where T_1 and T_2 are defined in Appendix I.

3.2 Effect of Eddy Currents on Power Amplifier

Using the method described in (ref. 6) the eddy current transfer function of the power amplifier is calculated to be

$$G_p(s) = \frac{1 + T_1 s}{1 + T_2 s} = \frac{1 + 0.1636 \times 10^{-3} s}{1 + 0.3085s}$$

The block diagram for the power amplifier including the inductance of the coil L, the eddy current transfer function $G_p(s)$, and the current i_c feedback is shown in Fig. 3,
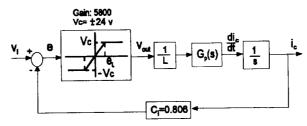

Figure 3. Block diagram showing power amplifier constraints and eddy current model transfer function.

where V_c is the maximum voltage of the power amplifier (V_c=24.0 V), C_i is the current feedback parameter (C_i=0.806), and e_L is the maximum error signal for linear operation of the power amplifier (e_L= V_c/gain= 24.0/5800).

3.3 Constraint Analysis for Power Amplifier

To understand the operation of the power amplifier consider diagram shown in Fig. 3.

The output voltage of the power amplifier is given by

$$V_{out} = \begin{cases} 5800e, & -e_L < e < +e_L \\ V_c, & |e| \geq e_L \end{cases}$$

(8)

From Eq. (8) we obtain

$$V_{out} = V_c sat\left(\frac{V_i - 0.806 i_c}{e_L}\right)$$

(9)

From Eq. (9), the equation for the current slew rate is given by

$$s\, i_c = \frac{1}{L} V_c sat\left(\frac{V_i - 0.806 i_c}{e_L}\right) G_p(s)$$

(10)

Eq. 10 shows that the maximum current slew rate is determined by the inductance L, the maximum error signal e_L for linear operation and the maximum output voltage V_c. Those equations are used for the simulation of the magnetic bearing system control.

4. SIMULATION AND EXPERIMENTAL RESULTS

To clarify the significance of the many assumptions in the theoretical analysis presented above, some experiments as well as simulations have been performed. The simulation work has been performed using the simulation software package Advanced Continuous Simulation Language (ACSL) for the system shown in Fig. 1. In this work the model used for the bearing actuator is given by Eqs. (1) to (6) and for the power amplifier is given by Eqs. (8) to (10). The

310

initial conditions in all simulations have been taken to be $x(0)=0.147$ mm and $i(0)=$ -0.1 A. Also in the simulation work, two different values of coil inductance L are used, these being 0.042 H and 0.072 H. The height b, of the solid core of linear ferromagnetic material has been taken to be 3 mm and 4 mm. In the experimental work, the coil inductance L is 0.042 H and the height b, of the solid core of linear ferromagnetic material is 3 mm. The simulation results show the system is stable for $7307 < C_x/C_i < 15275$. For $C_x=19140$ both the simulation and the experiments show the control system will have a limit cycle oscillation. The results of this work and their comparison are discussed below.

4.1 Simulation Results for Changes of the Coil Inductance L

In this section the control system coefficients are taken to be $C_x=19140$ and $b=3$ mm, and the system performance is examined for changing coil inductance L. Figs. 4 and 6 show the coil currents and the flywheel displacements waveforms of the magnetic bearing for $L=0.042$ H and $L=0.0567$ H, respectively. From the above figures, it will be noted that the coil current waveforms for the system simulation initially rise rapidly due to the effects of the eddy currents. The simulated dynamic response trajectories, in the i-x plane, for the bearing control system are shown in Figs. 5 and 7 with $L=0.042$ H and $L=0.0567$ H, respectively. There is a noticeable difference between their trajectories. The displacements waveforms of the system simulation for $L=0.042$ H dwell at the limits, $\pm x_m$, for only a very short period. However these is a considerable dwell time at the limits $\pm x_m$ when the coil inductance L is 0.0567 H.
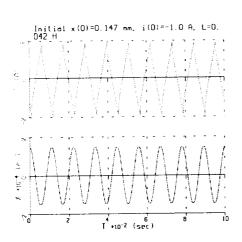

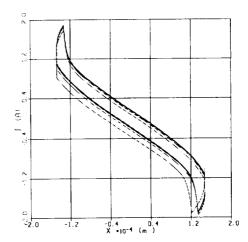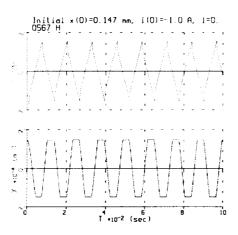Figure 4. Simulation time response for $C_x=19140$ and $L=0.042$H.

Figure 5. Simulation response trajectory in i-x plane for $C_x=19140$ and $L=0.042$H.

4.2 Simulation Results for Changes of the Eddy Current Transfer Function and the Controller Coefficients

In this section, the transfer function of the eddy currents has been changed to test the system stability, especially due to changes of the height b, of the solid core of

Figure 6. Simulation time response for C_x=19140 and L=0.0567H.

Figure 7. Simulation response trajectory in i-x plane for C_x=19140 and L=0.0567H.

linear ferromagnetic material and the gain coefficient C_x. All other coefficients are assumed fixed with L= 0.042 H and C_i= 0.806. The simulation results of the displacements and the currents for b= 4 mm and C_x= 8000 are shown in Figs. 8 and 9, respectively. From these figures it will be noted that the system is stable when changing the value b and the controller coefficients C_x. The simulation results show that the system should be stable for b=3 mm or b=4 mm and for $5889 < C_x < 12311$.
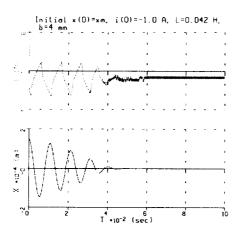

Figure 8. Simulation time response for C_x=19140, b=4 mm and L=0.042H.
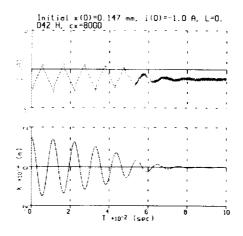

Figure 9. Simulation time response for b=3 mm, C_x=8000, and L=0.042H.

312

4.3 Experimental Results

In this section, the coil inductance L=0.042 H and the height of the solid core of linear ferromagnetic material b=3 mm for the experimental work. Fig. 10 shows the
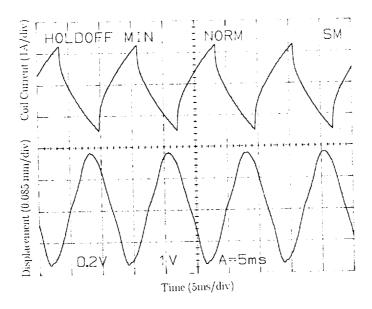

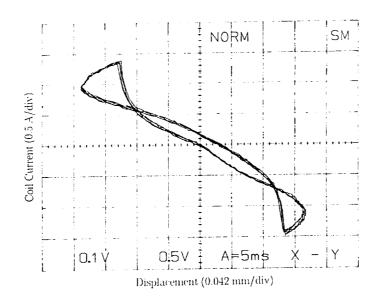Figure 10. Experimental time response for C_x=19140, b=3 mm and L=0.042H.

Figure 11. Experimental time response in i-x plane for C_x=19140, b=3 mm and L=0.042H.

313

experimentally measured coil current and flywheel displacement waveforms of the bearing and its control system for the controller coefficients C_x=19140 and C_i=0.806. The trajectory in the i-x plane for the same waveforms is shown In Fig. 11. The waveforms for the simulated system with the same operating conditions is shown in Figs. 4 and 5.

It is obvious that there is close correlation between the simulation and the experimental waveforms for L=0.042 H, C_x=19140 and b=3 mm. The coil current waveforms for the simulated system and the experimental system have a rapidly rising initial wavefront due to the effect of induced eddy currents. It will be noted that the results of the simulation using the eddy current model can predict the experimental results more accurately than the model without considering the eddy currents.

DISCUSSION

The large scale excited oscillations have been investigated and found to be due to a limit cycle which occurs in the magnetic bearing system. A simplified analysis of the magnetic bearing actuator and its control system, which includes the essential nonlinearities of the physical displacement constraints and the power amplifier saturation, has been undertaken. A useful design relationship in this work was obtained which shows that as the coil inductance decreases, the bearing control system becomes stable for a wider range of values of C_x. It has been observed that improved simulation results are obtained if the effects of the eddy currents on the operation of the bearing actuator and the power amplifier are included. The results of this investigation clearly indicate that reduction of the coil inductance not only improves the large signal operation of the magnetic bearing and prevents self-excited oscillations, but also significantly improves its disturbance robustness.

APPENDIX I. BEARING ACTUATOR MODEL

The transfer function of the magnetic bearing including the eddy currents is shown (ref. 6) to be

$$G_m(s) = \frac{x(s)}{I(s)} = -K_i \left(\frac{1 + T_2 s}{1 + T_1 s} \right) \frac{1}{Ms^2 + K}$$

where $T_1 = 4\delta\mu b^2/\pi^2$ and $T_2 = (1 - 8/\pi^2) T_1$. In these equations, δ is the plate conductivity

314

($\delta = 0.3571 \times 10^{-8}$ Ωm for steel), μ is the plate permeability ($\mu = \mu_r \mu_0$ where $\mu_0 = 4\pi \times 10^{-7}$ H/m), b is the height of the solid core of linear ferromagnetic material ($b = 3 \times 10^{-3}$ m), m is the mass of the shaft ($m = 0.6583$ kg), K_x is the bearing actuator static stiffness ($K_x = 171.3$ N/mm), and K_i is the bearing actuator current sensitivity ($K_i = 23.06$ N/A).

REFERENCES

1. Y. N. Zhuravlyov; A. Mikhail; and E. Lantto.: Inverse Problems of Magnetic Bearing Dynamics. *4th Inter. Symp. on Magnetic Bearings*, ETH Zurich, August, 1994, pp. 79-84.

2. K. N. Hirochika and Y. Segawa.: H^∞ Control of Milling AMB Spindle, *Fourth International Symposium on Magnetic Bearings.* ETH Zurich, Switzerland, August, 1994, pp. 23 - 26.

3. M. Fujita; K. Hatake; and F. Matsumura.: Loop Shaping Based Robust Control of a Magnetic Bearing. *IEEE Control System*, August, 1993, pp. 57-64.

4. R. B. Zmood; D. K. Anand; J. A. Kirk; and D. Pang.: The Behaviour of Magnetic Bearing Subjected to Large Disturbances. *RMIT Technical Report,* 1990, RMIT, Australia.

5. R. L. Stoll.: The Analysis of Eddy Currents. *Oxford University Press*, Oxford 1974.

6. R. B. Zmood; D.K. Anand; and J.A. Kirk.: The Influence of Eddy Currents on MagneticBearing Actuator Performance. *Proc. of IEEE*, Vol. 75, No. 2 (1987), pp. 259-260.